Synthesis, Culture Medium Stability, and *in vitro* and *in vivo* Zebrafish Embryo Toxicity of Metal-Organic Framework Nanoparticles

Àngels Ruyra, ⊥ [a,b] Amirali Yazdi, ⊥ [a] Jordi Espín, ⊥ [a] Arnau Carné-Sánchez,[a] Nerea Roher,[b] Julia Lorenzo,[b,c] Inhar Imaz,[a] and Daniel Maspoch*[a,d]

Full Papers

Abstract: Metal-organic frameworks (MOFs) are among the most attractive porous materials today. They have garnered great attention for their potential utility in many different areas such as gas storage, separation, catalysis and biomedicine. However, very little is known about the possible health or environmental risks of these materials. Here, the results of toxicity studies on sixteen representative uncoated MOF nanoparticles (nanoMOFs), which were assessed for cytotoxicity to HepG2 and MCF7 cells *in vitro*, and for toxicity to zebrafish embryos *in vivo*, are reported. Interestingly, there is a strong correlation between their *in vitro* toxicity and their *in vivo* toxicity. NanoMOFs were ranked according to their respective *in vivo* toxicity (in terms of the amount and severity of phenotypic changes observed in the treated zebrafish embryos), which varied widely. Altogether these results show different levels of toxicity of these materials, whereby leaching of solubilized metal ions plays a main role.

Introduction

Metal-organic frameworks (MOFs) are porous materials built from the controlled crystallization of metal ions or higher nuclearity metal clusters with multifunctional organic ligands.[1-3] When assembled at the nanoscale, they are called *nanoMOFs*. Analogously to other classes of nanoparticles, nanoMOFs show size-dependent properties (*e.g.* different adsorption kinetics or better dispersibility compared to their bulk analogs, *etc.*),[1] which can be exploited in numerous practical applications, including traditional storage⁴ and catalysis;[5,6] newer areas like sensors,[7]

functional membranes and thin-films;[8,9] and biomedical applications such as drug-delivery,[10-12] NO absorption[13,14] and contrast agents.[15] The ever-growing interest in nanoMOFs (and in their bulk analogs) should ultimately lead to their widespread production and use. However, little is known about the safety of these nanomaterials to humans and to the environment. Thus, before any nanoMOF can be adopted for practical use, its Environmental Health and Safety (EHS) profile must be determined.

Prior to the work we report here, other groups had already explored the *in vitro* toxicity of certain bare nanoMOFs in cells. In 2008, Lin *et al.* assayed the cytotoxicity of amorphous disuccinato-cisplatin/Tb(III) nanoparticles (size: ~ 60 nm) to HT-29 human colon adenocarcinoma cells, observing no appreciable cytotoxicity.[16] Starting in 2010, Horcajada, Gref, Serre *et al.* evaluated the *in vitro* toxicity of several Fe(III)-based nanoMOFs (*e.g.* nanoMIL-53, nanoMIL-88, nanoMIL-100, and nanoMIL-101; size: 90 nm to 200 nm) to various cell lines, including mouse macrophage J774.A1, human leukemia (CCRF-CEM), human multiple myeloma (RPMI-8226) and human cervical adenocarcinoma (HeLa) cells, generally finding low cytotoxicities.[10,17-20] Roughly in parallel, Junior *et al.* assayed nanoZIF-8 (size: 200 nm) against three human cell lines (mucoepidermoid carcinoma of lung [NCI-H292], colorectal adenocarcinoma [HT-29] and promyelocytic leukemia [HL-60]), and found that at the highest tested concentration (109 µM), it was not cytotoxic to any of them.[11] However, Horcajada *et al.* recently observed cytotoxicity of nanoZIF-8 (size: 90 nm) to HeLa and J774 cell lines, reporting IC_{50} values of 436 µM and 109 µM, respectively.[18] They also reported that Zr(IV)-based UiO-66 (size: 100 nm) was more toxic, showing IC_{50} values of 239 µM (HeLa) and 36 µM (J774).

The aforementioned results are from *in vitro* studies only. Importantly, the only *in vivo* studies on nanoMOFs reported to date were done in Wistar female rats.[10] In these studies, the rats were given one of three Fe(III)-based nanoMOFs (nanoMIL-88, nanoMIL-100 or nanoMIL-101) by intravenous injection, and subsequently analyzed for various parameters (*e.g.* serum, enzymatic, histological, etc.). The results revealed a lack of severe acute or sub-acute toxicity.

In this communication, we report combined *in vitro* (HepG2 and MCF7 cells) and *in vivo* (zebrafish embryos) studies on the toxicity of sixteen archetypical, uncoated nanoMOFs. As shown in Figure 1, the selected nanoMOFs comprise: **(1)** *MIL-100* [Fe₃O(H₂O)₂Cl(btc)₂], btc: 1,3,5-benzenetricarboxylic acid;[21] **(2)**

[a] À. Ruyra, A. Yazdi, J. Espín, A. Carné-Sánchez, Dr. I. Imaz, Prof. Dr. D. Maspoch
ICN2 (ICN-CSIC), Institut Catala de Nanociencia i Nanotecnologia
Esfera UAB, 08193 Bellaterra, Barcelona (Spain)
E-mail: daniel.maspoch@icn.cat
[b] À. Ruyra, Dr. N. Roher, Dr. J. Lorenzo
Institut de Biotecnologia i de Biomedicina – Parc de Recerca UAB
Campus Universitat Autònoma de Barcelona, 08193 Bellaterra, Barcelona (Spain)
[c] Dr. J. Lorenzo
Departament de Bioquímica i de Biologia Molecular
Campus Universitat Autònoma de Barcelona, 08193 Bellaterra, Barcelona (Spain)
[d] Prof. Dr. D. Maspoch
Institució Catalana de Recerca i Estudis Avançats (ICREA)
08100 Barcelona (Spain)
⊥ These authors contributed equally

Supporting information for this article is given via a link at the end of the document

MIL-101 [Fe$_3$Cl(H$_2$O)$_2$O(NH$_2$-bdc)$_3$], NH$_2$-bdc: 2-aminobenzene-1,4-dicarboxylic acid;[22] **(3)** *MOF-5* [Zn$_4$O(bdc)$_3$], bdc: 1,4-benzenedicarboxylic acid;[23] **(4-9)** the *MOF-74* (also called *CPO-27* family) [M$_2$(dhbdc)], M: Zn(II), Cu(II), Ni(II), Co(II), Mn(II), and Mg(II), dhbdc: 2,5-dihydroxy-1,4-benzenedicarboxylic acid;[24] **(10)** *ZIF-7* [Zn(Ph-im)$_2$], Ph-im: benzylimidazole;[25] **(11)** *ZIF-8* [Zn(Me-im)$_2$], Me-im: 2-methylimidazole;[25] **(12)** *UiO-66* [Zr$_6$O$_4$(OH)$_4$(bdc)$_6$]; **(13)** *UiO-66-NH$_2$* [Zr$_6$O$_4$(OH)$_4$(NH$_2$-bdc)$_6$];[26] **(14)** *UiO-67* [Zr$_6$O$_4$(OH)$_4$(bpdc)$_6$], bpdc: biphenyl-4,4′-dicarboxylic acid;[27] **(15)** *HKUST-1* [Cu$_3$(btc)$_2$];[28] and **(16)** *NOTT-100* (also called *MOF-505*) [Cu$_2$(bptc)], bptc: 3,3',5,5'-biphenyl-tetracarboxylic acid.[29]

We screened the nanoMOFs for cytotoxicity to the two aforementioned cell lines (using common *in vitro* methodologies), performed *in vivo* studies in zebrafish (as an *in vivo* model appropriate for comparative studies on mammalian biology), and finally, compared the results from each study. Zebrafish is recognized by the National Institute of Environmental Health Science (NIEHS, USA) and the Institute for Environment and Sustainability (IES, Europe) as an excellent system in which to study environmental toxicity,[29,30] and is accepted by the National Institutes of Health (NIH, USA) as an alternative model for exploring human diseases.[29-31] Besides, zebrafish embryo assays do not raise major ethical questions regarding vertebrate experimentation. Based on our results, we ranked the nanoMOFs according to their *in vivo* toxicity (in terms of amount and severity of phenotypic changes in the treated zebrafish embryos). We found that this ranking parallels the *in vitro* toxicity rankings for both cell lines, and that the toxicity

mM) for the *in vitro* and *in vivo* toxicity studies. Transmission Electron Microscopy (TEM) (Figure 1) and X-ray Powder Diffraction (XRPD) of the resulting colloids demonstrated that all selected nanoMOFs were obtained as homogeneous nanoscale crystals and that their XRPD patterns were fully coincident with the simulated patterns calculated from atomic coordinates (see Figure S1). In addition, all colloidal dispersions were characterized by Dynamic Light Scattering (DLS) to confirm the crystal size measured from the TEM images, as well as the homogeneity of each sample and the absence of any aggregation of the nanocrystals in solution (see Figures S2 and S3).

Stability of the nanoMOFs in culture medium.

We studied the stability of all the nanoMOFs in the culture medium containing 10% fetal bovine serum (FBS). Each nanoMOF colloid was separately dispersed in the medium at a final concentration of 10 mM, and then incubated at 37 ºC for 24 h. The resulting solids were then collected by centrifugation, dried, weighed and finally, characterized by XRPD.

Table 1. NanoMOFs classified according to their degradation in the culture medium containing 10% fetal bovine serum (FBS). Note that the concentration of the corresponding metal ions solubilized after the incubation of each nanoMOF at 37 ºC for 24 hours was determined by ICP-OES. The minimum percentage of degradation (deg$_{min}$(%)) was calculated as follows: deg$_{min}$(%) = ([M$_s$]·V·S)/n$_{MOF}$; where V is the volume of DMEM; S is the stoichiometric ratio of nanoMOF to metal ion; and n$_{MOF}$ is the number of moles of initial nanoMOF.
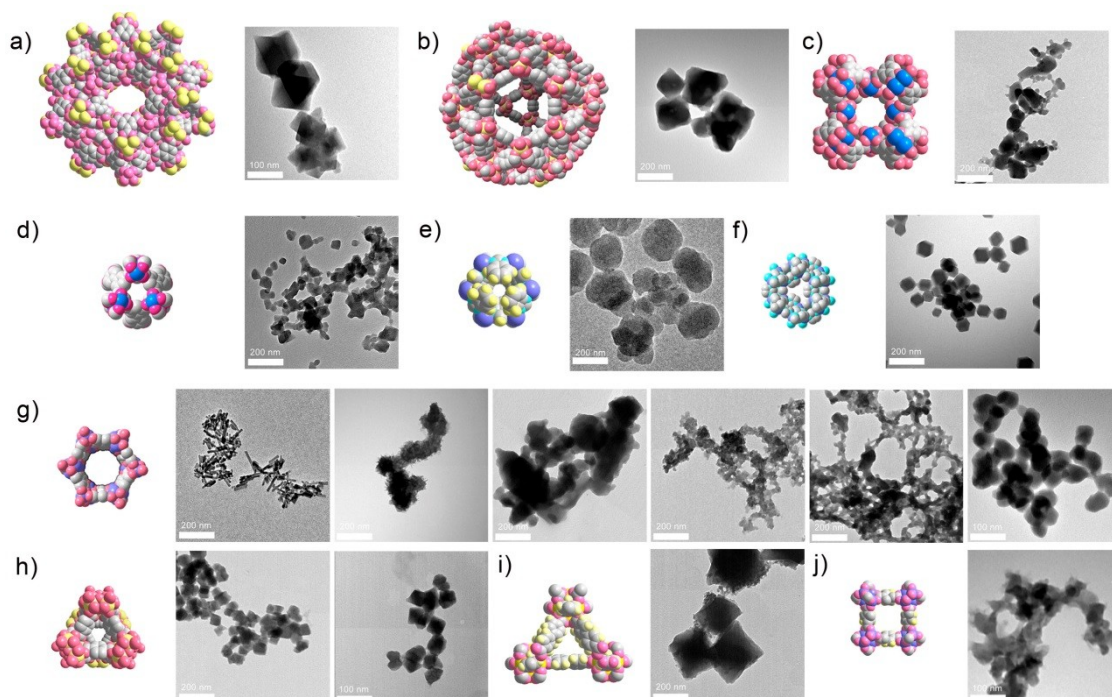
strongly depends on the solubility of the nanoMOFs and on their subsequent release of metal ions.

Once synthesized, all the nanoMOFs were cleaned to remove any impurities (including trace amounts of toxic solvents from the syntheses), dried at 80 ºC overnight, and finally, redispersed in DMSO to form stable colloids (concentrations: 25 mM to 100

nanoMOF	[M_s] (µM)	Degradation$_{min}$ (%)	XRPD Analysis
UiO-67	215.6 ± 6.3	0.3 ± 0.0	Amorphous
MIL-100	316.2 ± 46.1	1.1 ± 0.2	Stable
MIL-101	310.4 ± 90.1	1.1 ± 0.3	Amorphous
UiO-66	1099.8 ± 105.3	1.8 ± 0.2	Stable
UiO-66-NH₂	1567.5 ± 183.1	2.6 ± 0.3	Stable
ZIF-7	448.5 ± 23.4	4.5 ± 0.2	Stable
			...ity;
			... species (MnCO$_3$)
Co-MOF-74	3258.1 ± 58.8	16.2 ± 0.3	Loss of crystallinity
ZIF-8	1916.2 ± 75.4	19.1 ± 0.8	Stable
Zn-MOF-74	5442.6 ± 130.6	27.2 ± 0.5	Stable
HKUST-1	9168.6 ± 137.5	30.3 ± 0.5	Loss of crystallinity
Ni-MOF-74	7014.3 ± 174.9	35.1 ± 0.9	Stable
NOTT-100	7967.5 ± 152.8	39.4 ± 0.8	Loss of crystallinity
Cu-MOF-74	9556.8 ± 689.9	47.9 ± 3.4	Loss of crystallinity
Mg-MOF-74	12573.7 ± 273.9	62.9 ± 1.4	Loss of crystallinity

The robustness of the crystal structure of each nanoMOF was evaluated by comparing the initial and final XRPD spectra (see Figure S4). Also, the XRPD spectra were used to check for any other crystalline species that might have formed in the event that the nanoMOFs had degraded. Each supernatant was also characterized by Inductively Coupled Plasma-Optical Emission Spectrometry (ICP-OES) to estimate the amount of metal ion that had leaked from the nanoMOF and dissolved into the culture medium. Table 1 shows all the values extracted from this study. These data clearly indicate that all the nanoMOFs were at least partially soluble in the culture medium, although the degree of solubility varied widely by structure. The data also reveal that some of the nanoMOFs had become amorphous in the culture medium, having undergone structural rearrangements and/or reactions that generated new inorganic species.

The most soluble nanoMOF in culture medium was nanoMg-MOF-74 (12573 ± 274 µM Mg(II)$_s$; which corresponds to 62.9% of its constituent Mg(II)$_t$), and the least soluble, nanoUiO-67 (216 ± 6 µM Zr(IV)$_s$; which corresponds to 0.3% of its constituent Zr(IV)$_t$). Despite their vastly different levels of solubility, they each lost crystallinity and became amorphous upon contact with the culture medium.

NanoZIF-7 was poorly soluble in culture medium (449 ± 23 µM dissolved Zn(II)$_s$ ions, corresponding to 4.5% of its constituent Zn(II)$_t$), whereas nanoZIF-8 was more soluble, showing a leakage of 1916 ± 75 µM Zn(II)$_s$ (19.1% of its constituent Zn(II)$_t$). Interestingly, after incubation of each one in culture medium,

their respective crystal structures remained unaltered. NanoUiO-66 and nanoUiO-66-NH₂ also were very stable (see Figure S4), having released only 1100 ± 105 µM Zr(IV)$_s$ (1.8% of the constituent Zr(IV)$_t$) and 1568 ± 183 µM of Zr(IV)$_s$ (2.6% of the constituent Zr(IV)$_t$), respectively. In the case of nanoMIL-100 and nanoMIL-101, the concentrations of dissolved Fe(III) ions were only 316 ± 46 µM Fe(III)$_s$ (1.1% of the constituent Fe(III)$_t$) and 310 ± 90 µM (1.1% of the constituent Fe(III)$_t$), respectively. Although upon incubation both compounds became amorphous, upon subsequent exposure to ethanol, nanoMIL-100 recovered its crystallinity, which confirmed the robustness of its framework (see Figure S4).

The two Cu(II)-based nanoMOFs (nanoHKUST-1 and nanoNOTT-100) were relatively soluble, releasing 9169 ± 138 µM Cu(II)$_s$ (30.3% of its constituent Cu(II)$_t$) and 7968 ± 153 µM Cu(II)$_s$ (39.4% of its constituent Cu(II)$_t$). This degradation was clearly accompanied by a loss of crystallinity, which, in the XRPD patterns, is evidenced by the disappearance of most of the characteristic peaks. Similarly, the nanoM-MOF-74 family exhibited moderate to high solubility: nanoCu-MOF-74 released 9557 ± 690 µM Cu(II)$_s$ (47.9% of its constituent Cu(II)$_t$); nanoNi-MOF-74, 7014 ± 175 µM Ni(II)$_s$ (35.1% of its constituent Ni(II)$_t$); nanoZn-MOF-74, 5443 ± 131 µM Zn(II)$_s$ (27.2% of its constituent Zn(II)$_t$); nanoCo-MOF-74, 3258 ± 59 µM Co(II)$_s$ (16.2% of its constituent Co(II)$_t$); and nanoMn-MOF-74, 2651 ± 74 µM Mn(II)$_s$ (13.3% of its constituent Mn(II)$_t$). Upon incubation in the culture medium, all of these nanoMOFs suffered a loss of crystallinity, with nanoCuMOF-74, nanoCoMOF-74 and nanoMnMOF-74 exhibiting the greatest loss.

We would like to highlight that the proportion of metal ion (relative to the constituent amount of the tested nanoMOF) found in solution cannot always be directly related to the degradation of the nanoMOF. This is because degradation sometimes leads to formation of new, insoluble species. In our study, such species—provided that they were crystalline—were detectable by XPRD. Such was the case with nanoMn-MOF-74, whose XPRD spectrum after incubation in culture medium evidenced formation of MnCO$_3$ (see Figure S5). The formation of MnCO$_3$ was further studied by analyzing the powder resulting from the incubation, which confirmed the generation of new (rod-like) particles (see Figure S5). Electron-diffraction analysis (by TEM) of one of these particles revealed a diffraction pattern identical to that expected for MnCO$_3$ (see Figure S5). Formation of new species was also observed in the XRPD patterns for nanoCo-MOF-74, nanoMg-MOF-74 and nanoMOF-5. Unfortunately, in those cases, the new species could not be identified. NanoMOF-5 released 3108 ± 634 µM Zn(II)$_s$ (7.8% of its constituent Zn(II)$_t$), but its XRPD spectrum reveals the formation of a new, insoluble crystalline species, and lacks the characteristic peak of nanoMOF-5 itself (see Figure S4).

Given the above findings, we reasoned that the percentage of solubilized metal ions relative to the constituent amount of the tested nanoMOF represents the minimum percentage of degradation, as the ions might have further reacted to form insoluble species in the culture medium. Here, we would like to mention that four of the most structurally robust nanoMOFs

(nanoMIL-100, nanoMIL-101, nanoUiO-66 and nanoUiO-66-NH$_2$) actually underwent greater degradability in culture medium than that detected by analyzing the solubilized metal ions. In these cases, the weight-loss values (calculated by comparing the post- and pre-weight values, and expressed as a percentage) were much higher than were the corresponding values for relative percentage of solubilized metal ions: 25.8 ± 2.5% for nanoMIL-100 (1.1%); 10.3 ± 4.1% for nanoMIL-101 (1.1%); 14.7 ± 0.3% for nanoUiO-66 (1.8%); and 10.1 ± 0.8% for nanoUiO-66-NH$_2$ (2.6%). We have tentatively attributed these differences to insoluble, amorphous metal-containing species resulting from the reaction of the released metal ions in the cell culture media. In fact, this phenomenon has previously been observed for Zn(II) metal ions in cell culture media: for instance, ZnO nanoparticles have been reported to release Zn(II) into cell culture media or serum, which then rapidly reacts to form a poorly soluble, amorphous nanostructured Zn(II)-carbonate-phosphate precipitate.[35,36]

In vitro cytotoxicity of the nanoMOF components

The cytotoxicity of each organic ligand and each metal ion (as a chloride salt; except for MgSO$_4$) used to build the nanoMOFs was individually evaluated in HepG2 cells, using the XTT assay. The cells were exposed to a single organic ligand or metal salt at doses ranging from 1 µM to 200 µM for 24 h (see Figures S6 and S7). None of the organic ligands showed any significant cytotoxicity, even at the highest dose, nor did the Co(II), Ni(II), Zn(II), Zr(IV) or Mg(II) salts: cell viabilities were greater than 75% in all cases. Contrariwise, the Cu(II) and Mn(II) salts exhibited high cytotoxicity, even at low doses (5 µM to 10 µM); and Fe(III) showed moderate to high cytotoxicity from 25 µM to 200 µM, respectively.
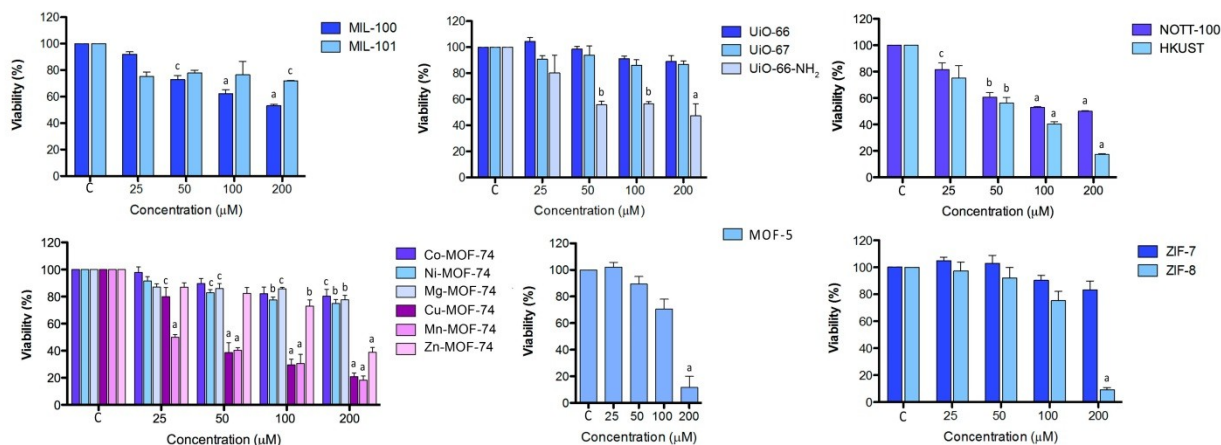
In vitro cytotoxicity of the nanoMOFs

The effect of each nanoMOF on cell viability was tested in HepG2 cells and in MCF7 cells using the XTT assay, at doses ranging from 25 µM to 200 µM, for 24 h and 72 h. Firstly, prior to the assay the DMSO colloid of a given nanoMOF was mixed with the cell culture medium. We would like to mention that the formation and use of these colloids is an intermediate but necessary step for minimizing any possible aggregation of nanoMOFs in the cell-culture medium. However, despite this step, many of the nanoMOFs still gradually agglomerated in both media, forming soft agglomerates. Thus, under these conditions, we were unable to differentiate between toxicity arising from single nanocrystals of each nanoMOF and toxicity arising from their corresponding agglomerates.

For most of the nanoMOFs, their respective cytotoxicity depended on the cell type and on the concentration (see Figures 2 and S8). Interestingly, some of the nanoMOFs (Co-MOF-74, Mg-MOF-74, UiO-66, and UiO-67) showed little or no cytotoxicity, even at the highest dose (200 µM). Within the nanoMOF-74 family, the cytotoxicity of each member varied

according to the metal component (Figure 2): those containing Co, Ni or Mg showed no marked cytotoxicity to either of the cell lines after 24 h of incubation, whereas those containing Cu, Mn or Zn showed high levels of cytotoxicity at the highest dose (200 µM). The viability levels observed in the cells exposed to the latter were 20.9 ± 2.7% (HepG2) and 38.2 ± 0.3% (MCF7) for nanoCu-MOF-74; 18.3 ± 3.0% (HepG2) and 32.4 ± 3.8% (MCF7) for nanoMn-MOF-74; and 38.8 ± 3.6% (HepG2) and 57.6 ± 0.6% (MCF7) for nanoZn-MOF-74. These results were generally consistent with those observed at 72 h (see Figure S8), although some differences were identified. For example, the cytotoxicity of nanoNi-MOF-74 to MCF7 cells was higher after 72 h, whereas that of nanoCu-MOF-74 to the same cells, and that of nanoZn-MOF-74 to HepG2 cells, were each lower after 72 h. NanoMIL-100 and -101 showed little or moderate toxicity to each cell line after 24 h and 72 h. However, at its highest dose (200 µM) and 24 h incubation, nanoMIL-100 provoked a substantial decrease (53.2 ± 1.0%) in the viability of the HepG2 cells. Also, after 72 h, nanoMIL-101 led to a decrease in the viability (41.8 ± 7.3%) of HepG2 cells. None of the nanoUiO MOFs exhibited substantial cytotoxicity at either incubation time, except for nanoUiO-66-NH$_2$: at the highest dose (200 µM) and 24 h incubation, it showed moderate cytotoxicity to HepG2 cells (47.2 ± 9.4% viability). The results for the nanoZIF family of MOFs varied widely: nanoZIF-7 was not cytotoxic to the HepG2 cells and moderately cytotoxic to the MCF7 cells, whereas nanoZIF-8 was highly cytotoxic to both. Both nanoHKUST-1 and nanoNOTT-100 were highly cytotoxic to both cell lines at both incubation times: for example, at 200 µM and 24 h incubation, nanoHKUST-1 was highly toxic to HepG2 cells (17.4 ± 0.5% viability). The only exception was nanoNOTT-100 at 200 µM after 24 h incubation in MCF7 cells (94.2 ± 4.0% viability). Lastly, at 200 µM and 24 h or 72 h incubation time, nanoMOF-5 was highly cytotoxic to both cell lines.

HepG2

MCF7
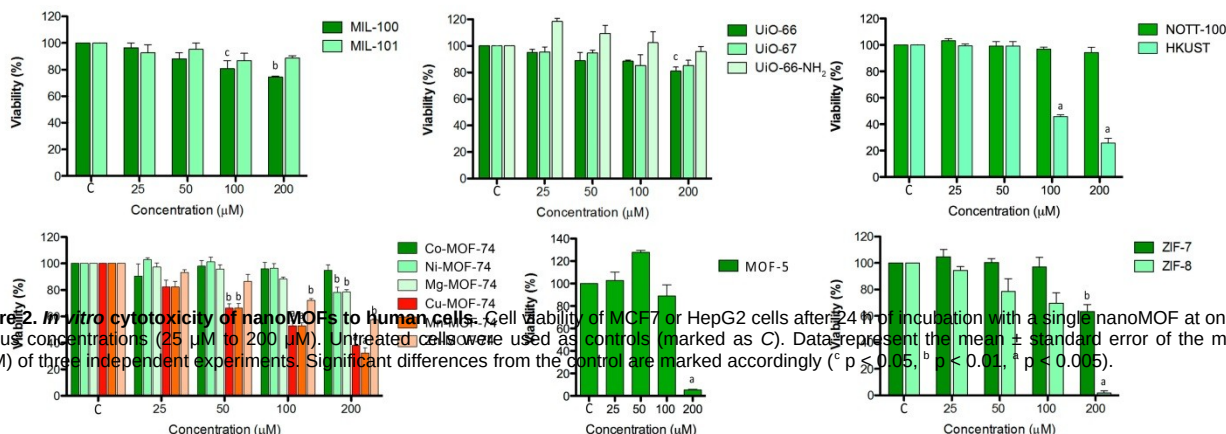
Figure 2. *In vitro* cytotoxicity of nanoMOFs to human cells. Cell viability of MCF7 or HepG2 cells after 24 h of incubation with a single nanoMOF at one of various concentrations (25 µM to 200 µM). Untreated cells were used as controls (marked as *C*). Data represent the mean ± standard error of the mean (SEM) of three independent experiments. Significant differences from the control are marked accordingly ([c] $p \leq 0.05$, [b] $p < 0.01$, [a] $p < 0.005$).

The toxicity of nanomaterials is widely accepted to derive from their chemical composition, through mechanisms such as dissolution and consequent release of toxic components (*e.g.* metal ions) or generation of reactive oxygen species, and/or to stress or stimuli caused by their surface reactivity, their size and/or their shape.[37] Albeit distinguishing amongst these mechanisms is not trivial, our results corroborate that the toxicity of nanoMOF crystals is at strongly related to their solubility and therefore, to their releasing of solubilized (toxic) metal ions.

The solubility tests on the sixteen nanoMOFs confirmed that they are all at least partially soluble in cell culture media and show minimum percentage of degradation in solution, ranging from 0.3% (nanoUiO-67) to 62.9% (nanoMg-MOF-74). This degradation induces the release of their constituent metal ions and organic ligands into the media.

Given that free metal ions, rather than free organic ligands, have previously been imputed as the toxic agents in MOFs,[18] we focused our attention on the metal ions solubilized in the media. Indeed, we found that the most cytotoxic nanoMOFs in our assays were those that released sufficiently high amounts of soluble metal ions known to be moderately or highly cytotoxic in their free form [*e.g.* Cu(II), Mn(II) and Fe(III)]. For example, nanoCu-MOF-74, nanoHKUST-1 and nanoNOTT-100, all of which are built from Cu(II) ions, were highly soluble and toxic in our tests. We believe that this toxicity, similarly to that observed with other soluble nanomaterials,[36-40] might be attributed to the release and subsequent cellular uptake of Cu(II) ions. For example, nanoCu-MOF-74 was highly cytotoxic and provoked a rapid toxic effect: at nanoCu-MOF-74 concentrations of 50 µM and 100 µM, and 24 h of incubation, the viability of treated HepG2 cells had decreased to ~40% and ~30%, respectively.

This result is consistent with our cytotoxicity studies on free Cu(II) ions (see Figure S6): for example, at a $Cu(II)_s$ concentration of 50 µM and 24 h of incubation, the viability of treated HepG2 cells had dropped to 23.9%. Assuming a similar rate of release of $Cu(II)_s$ over the entire range of concentrations, this viability value for Cu(II) alone corresponds to ~50 µM of nanoCu-MOF-74 (47.9% of constituent $Cu(II)_t$ lost; 38.7% cell viability for the same incubation time), ~55 µM of nanoHKUST-1 (30.3% of constituent $Cu(II)_t$ lost; cell viability: < 60%) and ~63 µM of nanoNOTT-100 (39.4% of constituent $Cu(II)_t$ lost; cell viability: < 60%) (see Figure 2). We observed a similar correlation between the cytotoxicity of free metal ions and the corresponding nanoMOFs in our studies on free Mn(II) ions and on nanoMn-MOF-74. At the lowest concentration (25 µM) and 24 h of incubation, this nanoMOF caused the viability of HepG2 cells to decrease to 49.9%. At this concentration, a release of ~ 3 µM $Mn(II)_s$ (13.3% of the constituent $Mn(II)_t$) would be expected, which would correlated to cell viabilities between 30% and 70%.

Unlike the aforementioned cases, the nanoMOFs that release significant amounts of soluble metal ions, but whose free constituent metal ion did not show cytotoxicity in the free form at the working concentrations [Co(II), Ni(II) or Mg(II)], showed little or no toxicity. These include nanoMg-MOF-74, nanoCo-MOF-74 and nanoNi-MOF-74. Similarly, those nanoMOFs that do not release significant amounts of soluble metal ions showed low cytotoxicity. These include nanoMIL-100, nanoMIL-101, nanoUiO-66, nanoUiO-66-NH₂, nanoUiO-67 and nanoZIF-7. The only exceptions to this trend were three of the Zn(II)-based nanoMOFs: nanoZn-MOF-74, nanoZIF-8 and nanoMOF-5. In all

three cases, we expected the concentration of $Zn(II)_S$ ions released from the nanoMOF to be lower than the maximum working concentration of 200 µM (at which free Zn(II) ions did not show any significant cytotoxicity; in fact, the *in vitro* toxic concentration of Zn(II) ions has been reported to be ~400 µM).[41] However, all three nanoMOFs caused high cytotoxicity at 200 µM. Interestingly, these results are consistent with recent studies on nanoIRMOF-3 that showed cytotoxicity to PC12 cells: in which cell viability was ~ 55% at 122 µM and < 20% at 488 µM.[42] They are also consistent with findings from studies on ZnO or Zn nanoparticles, whose toxicity could not be imputed solely to their release of Zn(II) ions into solution.[43] In fact, several authors have suggested that Zn nanoparticles might generate reactive oxygen species that induce oxidative stress[36,44-46] or that exhibit body burden or size effects; any of these factors might have contributed to the cytotoxicity that we observed in the Zn(II)-based nanoMOFs.
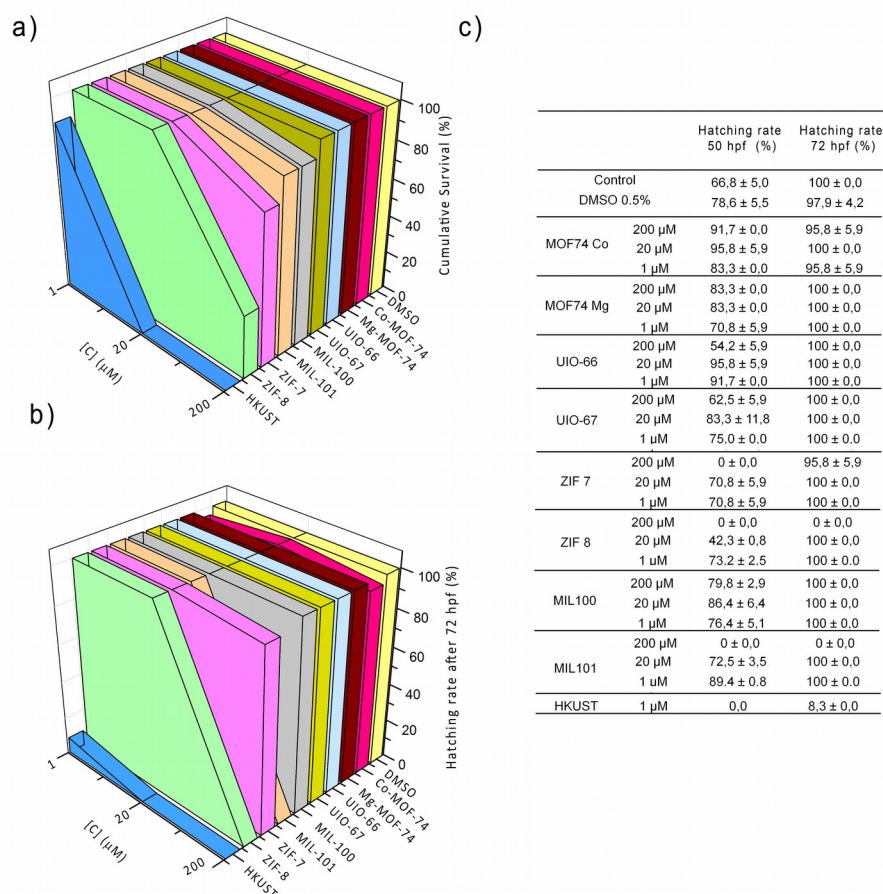
In vivo toxicity in zebrafish embryos

We then evaluated the *in vivo* toxicity of nine of the sixteen nanoMOFs in zebrafish (*Danio rerio*) embryo, and subsequently compared the results to those corresponding to the *in vitro* assays. Zebrafish embryo have been used extensively to assay the *in vivo* toxicity of nanoparticles because they are comparable to mammalian systems and amenable to medium-to-high-throughput screening.[47-50] Zebrafish embryos exposed to different concentrations (1 µM to 200 µM) of a suspension of a single nanoMOF were assessed for several toxicity parameters every 24 h until 120 h post-fertilization (hpf): these include mortality, hatching rate and appearance of abnormal phenotypes (*e.g.* low pigmentation, pericardial/yolk sac edema, delayed development, bent spine, *etc.*).

We chose nine nanoMOFs for *in vivo* evaluation to represent a wide spectrum of cytotoxicity from the *in vitro* assays, including non- or barely cytotoxic (nanoUiO-66, nanoUiO-67, and nanoCo-MOF-74 and nanoMg-MOF-74), moderately cytotoxic (nanoZIF-7, nanoMIL-100 and nanoMIL-101) and highly cytotoxic (nanoZIF-8 and nanoHKUST-1). In order to rule out any effects provoked by the 0.5% DMSO present in the three nanoMOF suspensions (1 µM, 20 µM and 200 µM), we also assessed its toxicity. At a final concentration of 0.5% in E3 medium, DMSO was found not to have any visible effects on normal larvae development after 120 h exposure: no differences in survival rate, hatching rate or phenotype were observed between the DMSO-treated group of larvae and the negative control (untreated) group.

Figure 3a shows the cumulative mortality of embryos from assay. We found that at 120 hpf, the vast majority of the nanoMOFs had not altered embryo viability. Hence, the viabilities of the embryos exposed to nanoCo-MOF-74, nanoMg-MOF-74, nanoUiO-66, nanoUiO-67, nanoMIL-100 and nanoMIL-101 were not significantly different to those of the control (DMSO-treated) group. Contrariwise, nanoZIF-7, nanoZIF-8 and nanoHKUST-1 provoked significant decreases in embryo survival (Figures 3 and S9). NanoZIF-7 was slightly toxic at 200 µM (embryo viability at 120 hpf: 79.2%); nanoZIF-8 was more toxic at the same concentration (embryo viability at 120 hpf: 33.3%); and nanoHKUST-1 was extremely toxic at this concentration (viability: 0%); in fact, even at 20 µM nanoHKUST-1, none of the embryos treated with this nanoMOF had survived by 48 hpf (viability: 0%).

a)

b)

c)

|		Hatching rate 50 hpf (%)	Hatching rate 72 hpf (%)
Control		66,8 ± 5,0	100 ± 0,0
DMSO 0.5%		78,6 ± 5,5	97,9 ± 4,2
MOF74 Co	200 µM	91,7 ± 0,0	95,8 ± 5,9
	20 µM	95,8 ± 5,9	100 ± 0,0
	1 µM	83,3 ± 0,0	95,8 ± 5,9
MOF74 Mg	200 µM	83,3 ± 0,0	100 ± 0,0
	20 µM	83,3 ± 0,0	100 ± 0,0
	1 µM	70,8 ± 5,9	100 ± 0,0
UIO-66	200 µM	54,2 ± 5,9	100 ± 0,0
	20 µM	95,8 ± 5,9	100 ± 0,0
	1 µM	91,7 ± 0,0	100 ± 0,0
UIO-67	200 µM	62,5 ± 5,9	100 ± 0,0
	20 µM	83,3 ± 11,8	100 ± 0,0
	1 µM	75,0 ± 0,0	100 ± 0,0
ZIF 7	200 µM	0 ± 0,0	95,8 ± 5,9
	20 µM	70,8 ± 5,9	100 ± 0,0
	1 µM	70,8 ± 5,9	100 ± 0,0
ZIF 8	200 µM	0 ± 0,0	0 ± 0,0
	20 µM	42,3 ± 0,8	100 ± 0,0
	1 uM	73,2 ± 2.5	100 ± 0,0
MIL100	200 µM	79,8 ± 2,9	100 ± 0,0
	20 µM	86,4 ± 6,4	100 ± 0,0
	1 µM	76,4 ± 5,1	100 ± 0,0
MIL101	200 µM	0 ± 0,0	0 ± 0,0
	20 µM	72,5 ± 3,5	100 ± 0,0
	1 uM	89,4 ± 0.8	100 ± 0,0
HKUST	1 µM	0,0	8,3 ± 0,0

Figure 3. *In vivo* toxicity of nanoMOFs to zebrafish embryos. (a) Cumulative survival of zebrafish larvae at 120 h post-fertilization (hpf) after exposure to a single nanoMOF at one of three concentrations (1 µM, 20 µM or 200 µM). (b) Concentration-dependent (1 µM, 20 µM or 200 µM) effects of nanoMOFs on the hatching rates of zebrafish embryos at 120 hpf. (c) Quantification of hatching rates (%) at 50 hpf and 72 hpf.

We quantified the hatching rate of the embryos in the nanoMOF-treated group and the control group. As shown in Figures 3b and 3c, some of the nanoMOF-treated group exhibited a significant concentration-dependent hatching delay. Many previous studies have reported that fish embryos exposed to nanoparticles exhibit delayed hatching,[40,47,51] although whether this delay is caused by the whole nanoparticles themselves or by their released constituent materials remains unknown.[52,53] Some researchers have proposed that the delay might be caused by interactions between the nanoparticles and the zebrafish hatching enzyme, which is crucial for digesting the inner layer of the chorion (the membrane surrounding the embryo).[52,54]

When incubated under normal conditions, control embryos hatched from their chorion between 48 hpf and 72 hpf (Figure 3c), exhibiting slightly accelerated hatching similarly to an effect that has been previously reported elsewhere.[55] However, the embryos incubated with nanoZIF-7 or nanoHKUST-1 hatched significantly later than did the control embryos (Figures 3b, 3c and S10), and of these two treated groups, only the nanoZIF-7 group reached 100% hatching rate. In the case of nanoHKUST-1, the hatching delay was only quantified at a nanoHKUST-1 dose of 1 µM, as no embryos survived at the higher doses. Interestingly, embryos exposed to the highest dose (200 µM) of nanoZIF-8 or nanoMIL-101 did not hatch at all by 120 hpf. It is important to mention here that nanoZIF-8 has an effect on the survival at this highest dose (200 µM). No significant hatching delay was observed in the groups exposed to nanoCo-MOF-74, nanoMg-MOF-74, nanoUiO-66, nanoUiO-67 or nanoMIL-100.

To further characterize the *in vivo* toxicity of nanoMOFs, we also quantified the morphological defects observed on the treated embryos after they had hatched (Figures 4 and S11). No significant malformations were found in the embryos that had been exposed to nanoMg-MOF-74; significant levels of yolk sac edema were found in the nanoCo-MOF-74, nanoUiO-66, nanoUiO-67 and nanoZIF-7 groups; concentration-dependent yolk sac edemas and significant pericardial edema was found in the nanoMIL-100 group. No further putative morphological defects could be detected in the groups exposed to 200 µM of nanoZIF-8 or nanoMIL-101, due to their inability to hatch, although some morphological malformations were observed in the groups exposed to lower doses of nanoZIF-8 (pericardial edema, yolk-sac edema and bent spine) or nanoMIL-101 (yolk sac edema) (see Figure S11). Interestingly, significant levels of pericardial edema, yolk-sac edema and bent spine were observed in the group that had been exposed to nanoHKUST-1 at the low dose of 1 µM; however, the malformations in the groups exposed to higher doses were not characterized, as none of the embryos had survived.
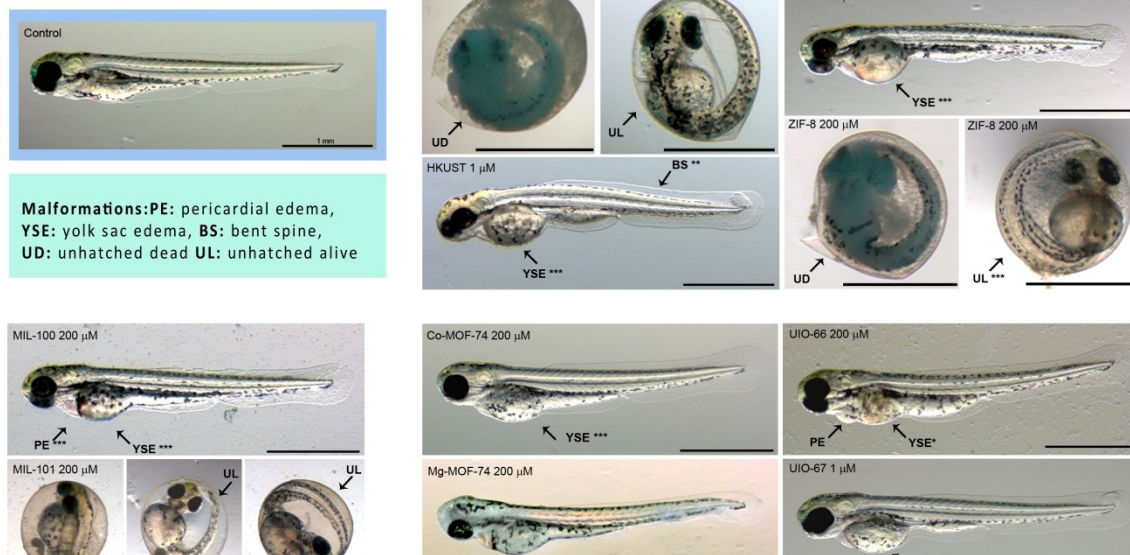
Figure 4. Malformations in zebrafish embryos that had been exposed to nanoMOFs. Representative images embryos were taken after continuous exposure to nanoMOFs (72 hpf). The malformations were imaged and quantified. Significant differences from the control are marked accordingly (**p < 0.01, *** p < 0.005).

Ranking of the *in vivo* toxicity of nanoMOFs

To compare the *in vivo* toxicity of the nine studied nanoMOFs, we quantified their *in vivo* effects on the zebrafish embryos using a scoring system that was first described by Peterson *et al.*[56,30] and subsequently modified by Nel *et al.*[47] Thus, we scored the amount and severity of the phenotypic changes, on a scale from 0 to 4, whereby 0 = *normal phenotype*; 1 = *a minor phenotypic change*; 2 = *multiple moderate alterations*; 3 = *severe embryo deformation*; and 4 = *no survival* (see Table 2). The nanoMOFs scored as follows: **0** (nanoMg-MOF-74); **1** (nanoCo-MOF-74, nanoUiO-66 and nanoUiO-67); **2** (nanoMIL-100 and nanoZIF-7); **3** (nanoZIF-8 and nanoMIL-101); and **4** (nanoHKUST-1).

Conclusions

We have assessed the *in vitro* toxicity and *in vivo* toxicity of a series of representative, uncoated, nanoscale metal-organic frameworks (nanoMOFs). We first screened sixteen nanoMOFs against two human cell lines (HepG2 and MCF7), and then screened a diverse set of nine of these nanoMOFs in zebrafish embryos. We found a strong correlation between the *in vitro* toxicity results and the *in vivo* toxicity results, with nanoMg-MOF-74 being the least toxic in both assays. The only exception to this trend was nanoMIL-101, which was relatively more toxic to

Table 2. Ranking of nanoMOFs by *in vivo* toxicity, according to a semi-quantitative scoring system (adapted from Nel *et al.*, 2011; and Furgeson *et al.*, 2009).

Score	Attributes	nanoMOF	Morphological defects	Physiological defects
0	No morphological or physiological defects	nanoMg-MOF-74		
1	Single morphological/ physiological defect	nanoCo-MOF-74, nanoUiO-66 and nanoUiO-67	yolk sac edema	
2	Multiple morphological and physiological defects	nanoMIL-100 and nanoZIF-7	pericardial and yolk sac edema, bent spine	mortality, reduced hatching rate
3	Severe multiple morphological and physiological defects	nanoMIL-101 and nanoZIF-8	pericardial and yolk sac edema, bent spine	mortality, embryos failed to hatch
4	Embryos do not survive	nanoHKUST-1	disintegrated embryo	

Comparison of the *in vitro* toxicity and the *in vivo* toxicity results for the nanoMOFs

We found a strong correlation between the *in vitro* toxicity results and the *in vivo* toxicity results for the nine nanoMOFs that we had tested in both assays (Table 3). The only deviation from this trend was that observed for nanoMIL-101, which was relatively more toxic to zebrafish embryos (adverse effect on hatching) than it was to HepG2 or MCF7 cells.

embryos than to cell cultures. Our findings suggest that degradation of nanoMOFs in solution generates metal ions that strongly determine the toxicity of these nanomaterials. However, other factors might also influence the toxicity of nanoMOFs, including the formation of other species upon degradation, or certain crystal parameters (*e.g.* size, shape, charge, *etc.*). We affirm that more studies on the possible environmental and health risks of nanoMOFs must be performed before these new nanomaterials can be exploited for practical use.

Table 3. Qualitative comparison between the *in vitro* and *in vivo* toxicity of the nanoMOFs studied in both assays.

Grade of toxicity	*In vitro*	*In vivo*
-	nanoMg-MOF-74, nanoCoMOF-74, nanoUiO-66 and nanoUiO-67	(0) nanoMg-MOF-74
+		(1) nanoCoMOF-74, nanoUiO-66 and nanoUiO-67
++	nanoMIL-100, nanoZIF-7 and nanoMIL-101	(2) nanoMIL-100 and nanoZIF-7
+++	nanoZIF-8	(3) nanoZIF-8 and nanoMIL-101
++++	nanoHKUST-1	(4) nanoHKUST-1

Experimental Section

Materials

All reagents and solvents used in the nanoMOF syntheses were purchased from Sigma-Aldrich and Romil, respectively, and were used without any further purification.

NanoMOF synthesis

The nanoMOFs were prepared using modified versions of methods from the literature. The general procedures are listed in the Supporting Information.

NanoMOF characterization

We characterized the synthesized nanoMOFs by X-ray Powder Diffraction (XRPD), to determine their purity, and by Transmission Electron Microscopy (TEM), Field-Emission Scanning Electron Microscopy (FESEM) and Dynamic Light Scattering (DLS), to determine their size distribution.

Stability studies

A carefully weighed sample of each nanoMOF was separately dispersed in 10 mL of DMEM medium with 10% FBS to achieve a final concentration of 10 mM. Each mixture was incubated at 37 °C for 24 h with gentle stirring, and then centrifuged for 5 min at 10000 rpm (Alegra 64R, Beckman Coulter). Each supernatant was characterized by Inductively Coupled Plasma-Optical Emission Spectroscopy (ICP-OES) in an Optima 4300DV™ unit (Perkin Elmer) to determine the amount of solubilized metal ions. In parallel, each pellet was washed with 10 mL of deionized water to remove buffer salts, and then centrifuged. This process was repeated with methanol, and the resulting solids were dried in an oven at 90 °C overnight, weighed and finally, characterized by XRPD. All the experiments were done in triplicate.

Evaluation of the *in vitro* toxicity of the nanoMOFs and their constituent components to HepG2 and MCF7 cells

Human hepatocyte (HepG2) and breast cancer (MCF7) cell lines were separately incubated with a single nanoMOF, and then the effects of the nanoMOFs on cell viability were assessed using the XTT (2,3-Bis-(2-Methoxy-4-Nitro-5-Sulfophenyl)-2*H*-Tetrazolium-5-Carboxanilide) cell viability assay[57] after 24 h and 72 h incubation time. The cells were cultured in either DMEM (Dulbecco's Modified Eagle's Medium, Invitrogen; for HepG2 cells) or DMEM F12 (for MCF7 cells), containing GlutaMax 1 and supplemented with 10% (v/v) heat-inactivated fetal bovine serum (FBS) (Invitrogen) at 37 ºC, 5% CO_2 and 95% humidity. The cells were seeded into 96-well plates (cell density: 4.0×10^3 cells/well), incubated for 24 h, and then exposed to fresh medium containing a DMSO suspension of the desired nanoMOF (concentrations: 25 to 200 µM). At 24 h and 72 h incubation, aliquots of 20 µL of XTT solution were added to each well, and the resulting color was quantified (λ = 450 nm) in a spectrophotometric plate-reader (Perkin Elmer Victor3 V). Cell viability was expressed as a percentage of the control level. All the measurements were done in triplicate, in three independent experiments. The same procedure was employed to separately evaluate the cytotoxicity of each nanoMOF component (metal salt or organic ligand) to HepG2 cells, except at a concentration range from 1 µM to 200 µM and at 24 h incubation time. Differences among the data were analyzed using one-way ANOVA, followed by Tukey's post test ($p < 0.001$).

Exposure of zebrafish embryos to nanoMOFs

Adult zebrafish (*Danio rerio*) were maintained in tanks with recirculating water under a 14 h light/10 h dark cycle at 28 ºC. Male and female zebrafish were set up in pairs for breeding in breeding tanks. A grid insert in the tanks enabled the resulting embryos to fall to the bottom avoiding parental predation. The embryos were collected in E3 medium (5 mM NaCl, 0.17 mM KCl, 0.33 mM $CaCl_2$, 0.33 mM $MgSO_4$ and 0.1% Methylene Blue), rinsed carefully to remove debris, and kept at 28 ºC in an incubator. The embryos were visually assessed with a microscope (Olympus, CKX31, Japan) for viability and developmental stage, and the selected healthy specimens were plated into 96-well plates at 1 embryo/well. Starting at 5 h post-fertilization, the embryos were exposed to 200 µL/well of: a solution of a single nanoMOF at different concentrations (1 µM, 20 µM and 200 µM; final concentration of DMSO in E3 medium: 0.5%); to a DMSO control solution (0.5% DMSO in E3 medium); or to E3 medium alone (negative control). The embryos were assessed for hatching rate, cumulative mortality and malformations at 24 h, 48 h, 72 h, 96 h and 120 hpf. Screening for morphological defects included the assessment of

abnormally developed eyes; lack of somite formation; delayed development; pericardial edema; yolk-sac edema; irregular pigmentation; tail malformation; and/or a bent spine. The most frequently found malformations (pericardial edema, yolk-sac edema and bent spine), were quantified. Embryos with abnormal morphologies were anaesthetized with ethyl 3-aminobenzoate methanesulfonate (160 ppm MS-222, Sigma), transferred onto microscope slides, and then photographed in a Leica Stereomicroscope MZ FLIII. Each condition was tested in 24 individuals. All experimental procedures were submitted to the Ethical Committee of the Universitat Autònoma de Barcelona, whose procedures follow the International Guiding Principles for Research Involving Animals.

Acknowledgements

[1] A. Carné, C. Carbonell, I. Imaz, D. Maspoch, *Chem. Soc. Rev.* **2011**, *40*, 291-305.

[2] H. Furukawa, K. E. Cordova, M. O'Keeffe, O. M. Yaghi, *Science* **2013**, *341*, 974-980.

[3] W. Lin, W. J. Rieter, K. M. L. Taylor, *Angew. Chem. Int. Ed.* **2009**, *48*, 650-658.

[4] D. Tanaka, A. Henke, K. Albrecht, M. Moeller, K. Nakagawa, S. Kitagawa, J. Groll, *Nat. Chem.* **2010**, *2*, 410-418.

[5] K. H. Park, K. Jang, S. U. Son, D. A. Sweigart, *J. Am. Chem. Soc.* **2006**, *128*, 8740-8741.

[6] L. J. Zhang, F. L. Jiang, Y. F. Zhou, W. T. Xu, M. C. Hong, *Tetrahedron* **2013**, *69*, 9237-9244.

[7] W. J. Rieter, K. M. L. Taylor, W. Lin, *J. Am. Chem. Soc.* **2007**, *129*, 9852-9853.

[8] T. Rodenas, M. van Dalen, E. García-Pérez, P. Serra-Crespo, B. Zornoza, F. Kapteijn, J. Gascon, *Adv. Funct. Mater.* **2014**, 24, 249-256.

[9] Y.-S. Li, H. Bux, A. Feldhoff, G.-L. Li, W.-S. Yang, J. Caro, *Adv. Mater.* **2010**, *22*, 3322-3326.

[10] a) P. Horcajada, T. Chalati, C. Serre, B. Gillet, C. Sebrie, T. Baati, J.F. Eubank, D. Heurtaux, P. Clayette, C. Kreuz, J. S. Chang, Y.-K. Hwang, V. Marsaud, P. N. Bories, L. Cynober, S. Gil, G. Ferey, P. Couvreur, R. Gref, *Nat. Mater.* **2010**, *9*, 172-178. b) W. Morris, W. E. Briley, E. Auyeung, M. D. Cabezas, C. A. Mirkin, *J. Am. Chem. Soc.* **2014**, *136*, 7261-7264.

[11] I. B. Vasconcelos, T. G. da Silva, G. C. G. Militao, T. A. Soares, N. A. Rodrigues, M. O. Rodrigues, N. B. da Costa Jr., R. O. Freire, S. A. Junior, *RSC Adv.* **2012**, *2*, 9437-9442.

[12] J. Zhuang, C.-H. Kuo, L.-Y. Chou, D.-Y. Liu, E. Weerapana, C.-K. Tsung, *ACS Nano* **2014**, *8*, 2812-2819.

[13] S. Diring, D. O. Wang, C. Kim, M. Kondo, Y. Chen, S. Kitagawa, K.-I. Kamei, S. Furukawa, *Nat. Commun.* **2013**, *4*, 2684-2684.

[14] N. J. Hinks, A. C. McKinlay, B. Xiao, P. S. Wheatley, R. E. Morris, *Micropor. Mesopor. Mater.* **2010**, *129*, 330-334.

[15] a) J. Della Rocca, W. Lin, *Eur. J. Inorg. Chem.* **2010**, 3725-3734. b) G. A. Pereira, J. A. Peters, F. A. Almeida Paz, J. Rocha, C. F. G. C. Geraldes, *Inorg. Chem. 2***010**, 49, 2969-2974. c) A. Foucault-Collet, K. A. Gogick, K. A. White, S. Villette, A. Pallier, G. Collet, C. Kieda, T. Li,

S. J. Geib, N. L. Rosi, S. Petoud, *Proc. Natl. Acad. Sci.* **2013**, DOI: 10.1073/pnas.1305910110. d) A. Carné-Sánchez, C. S. Bonnet, I. Imaz, J. Lorenzo, É. Tóth, D. Maspoch, *J. Am. Chem. Soc.* **2013**, *135*, 17711-17714.

[16] W. J. Rieter, K. M. Pott, K.M. L. Taylor, W. Lin, *J. Am. Chem. Soc.* **2008**, *130*, 11584-11585.

[17] T. Baati, L. Njim, F. Neffati, A. Kerkeni, M. Bouttemi, R. Gref, M. F. Najjar, A. Zakhama, P. Couvreur, C. Serre, P. Horcajada, *Chem. Sci.* **2013***, 4*, 1597-1607.

[18] C. Tamames-Tabar, D. Cunha, E. Imbuluzqueta, F. Ragon, C. Serre, M. J. Blanco-Prieto, P. Horcajada, *J. Mater. Chem. B.* **2014,** *2*, 262-271.

[19] T. Chalati, P. Horcajada, P. Couvreur, C. Serre, M. Ben Yahia, G. Maurin, R. Gref, *Nanomedicine* **2011**, *6*, 1683-1695.

[20] P. Horcajada, R. Gref, T. Baati, P. K. Allan, G. Maurin, P. Couvreur, G. Férey, R. Morris, C. Serre, *Chem. Rev.* **2012**, *112*, 1232-1268.

[21] P. Horcajada, S. Surble, C. Serre, D.-Y. Hong, Y.-K. Seo, J. S. Chang, J. M. Grenèche, *Chem. Commun.* **2007**, 2820-2822.

[22] S. Bauer, C. Serre, T. Devic, P. Horcajada, J. Marrot, G. Férey, N. Stock, *Inorg. Chem.* **2008**, *47*, 7568-7576.

[23] B. Chen, M. Eddaoudi, S. T. Hyde, M. O'Keeffe, O. M. Yaghi, *Science* **2001**, *291*, 1021-1023.

[24] N. L. Rosi, J. Kim, M. Eddaoudi, B. Chen, M. O'Keeffe, O. M. Yaghi, *J. Am. Chem. Soc.* **2005**, *127*, 1504-1518.

[25] K. S. Park, Z. Ni, A. P. Côte, J. Y. Choi, R. Huang, F. J. Urbe-Romo, H. K. Chae, M. O'Keeffe, O. M. Yaghi, *Proc. Natl. Acad. Sci. USA* **2006**, *103*, 10186-10191.

[26] J. H. Cavka, S. Jakobsen, U. Olsbye, N. Guillou, C. Lamberti, S. Bordiga, K. P. Lillerud, *J. Am. Chem. Soc.* **2008***, 130*, 13850-13851.

[27] S. S.-Y. Chui, S. M.-F. Lo, J. P. H. Charmant, A. G. Orpen, I. D. Williams, *Science* **1999**, *283*, 1148-1150.

[28] B. Chen, N. W. Ockwig, A. R. Millward, D. S. Contreras, O. M. Yaghi, *Angew. Chem. Int. Ed.* **2005,** *44*, 4745-4749.

[29] C. Parng, *Curr. Opin. Drug Discovery Dev.* **2005**, *8*, 100-106.

[30] O. Bar-Ilan, R. M. Albrecht, V. E. Fako, D. Y. Furgeson, *Small* **2009**, *5*, 1897-1910.

[31] S. Lin, Y. Zhao, A. E. Nel, S. Lin, *Small* **2013**, *9*, 1608-1618.

[32] M. Sindoro, N. Yanai, A.-Y. Jee, S. Granick, *Acc. Chem. Res.* **2013**, *47*, 459-469.

[33] J. Della Rocca, D. Liu, W. Lin, *Acc. Chem. Res.* **2011**, *44*, 957-968.

[34] A. Carné-Sánchez, I. Imaz, M. Cano-Sarabia, D. Maspoch, *Nat. Chem.* **2013,** *5*, 203-211.

[35] T. W. Turney, M. B. Duriska, V. Jayaratne, A. Elbaz, S. J. O'Keefe, A. S. Hastings, T. J. Piva, P. F. A. Wright, B. N. Feltis, *Chem. Res. Toxicol.* **2012,** *25*, 2057-2066.

[36] C. Shen, S. A. James, M. D. de Jonge, T. W. Turney, P. F. A. Wright, B. N. Feltis, *Toxicol. Sci.* **2013**, *136*, 120-130.

[37] T. J. Brunner, P. Wick, P. Manser, P. Spohn, R. N. Grass, L. K. Limbach, A. Bruinink, W. J. Stark, *Environ. Sci. Technol.* **2006,** *40*, 4374-4381.

[38] Y.-N. Chang, M. Zhang, L. Xia, J. Zhang, G. Xing, *Materials* **2012**, *5*, 2850-2871.

[39] M. Ates, J. Daniels, Z. Arslan, I. O. Farah, H. F. Rivera, *Environ. Sci.: Processes Impacts* **2013**, *15*, 225-233.

[40] W. Bai, Z. Zhang, W. Tian, X. He, Y. Ma, Y. Zhao, Z. Chai, *J. Nanopart. Res.* **2010**, *12*, 1645-1654.

[41] R. D. Palmiter, *Proc. Natl. Acad. Sci. USA* **2004,** *101*, 4918-4923.

[42] F. Ren, B. Yang, J. Cai, Y. Jiang, J. Xu, S. Wang, *J. Hazard. Mater.* **2014**, *271*, 283-291.

[43] V. Valdiglesias, C. Costa, G. Kiliç, S. Costa, E. Pásaro, B. Laffon, J. P. Teixeira, *Environ. Int.* **2013**, *55*, 92-100.

[44] A. Nel, T. Xia, L. Mädler, N. Li, *Science* **2006,** *311*, 622-627.

[45] T. Xia, M. Kovochich, J. Brant, M. Hotze, J. Sempf, T. Oberley, C. Sioutas, J. I. Yeh, M. R. Wiesner, A. E. Nel, *Nano Lett.* **2006**, *6*, 1794-1807.

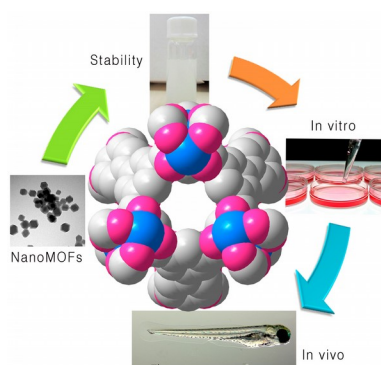[46] J. She, Z. Xiao, Y. Yang, S. Deng, J. Chen, G. Yang, N. Xu, *ACS Nano* **2008**, *2*, 2015-2022.

[47] S. George, T. Xia, R. Rallo, Y. Zhao, Z. Ji, S. Lin, X. Wang, H. Zhang, B. France, D. Schoenfeld, R. Damoiseaux, R. Liu, S. Lin, K. A. Bradley, Y. Cohen, Nel, A. *ACS Nano* **2011,** *5*, 1805-1817.

[48] X. Zhao, K. J. Ong, J. D. Ede, J. L. Stafford, K. W. Ng, G. G. Goss, S. C. J. Loo, *Small* **2013,** *9,* 1734-1741.

[49] B. J. Shaw, R. D. Handy, *Environ. Int.* **2011**, *37,* 1083-1097.

[50] S. Lin, X. Wang, Z. Ji, C. H. Chang, Y. Dong, H. Meng, Y.-P. Liao, M. Wang, T.-B. Song, S. Kohan, T. Xia, J. I. Zink, S. Lin, A. E. Nel, *ACS Nano* **2014**, *8*, 4450-4464.

[51] J. Cheng, E. Flahaut, S. H. Cheng, *Environ. Toxicol. Chem.* **2007**, *26*, 708-716.

[52] T. Xia, Y. Zhao, T. Sager, S. George, S. Pokhrel, N. Li, D. Schoenfeld, H. Meng, S. Lin, X. Wang, M. Wang, Z. Ji, J. I. Zink, L. Mädler, V. Castranova, S. Lin, A. E. Nel, *ACS Nano* **2011***, 5,* 1123-1235.

[53] X. Zhu, J. Wang, X. Zhang, Y. Chang, Y. Chen, *Nanotechnology* **2009**, *20*, 195103-195112.

[54] K. J. Ong, X. Zhao, M. E. Thistle, T. J. MacCormack, R. J. Clark, G. Ma, Y. Martinez-Rubi, B. Simard, J. S. C. Loo, J. G. C. Veinot, G. G. Goss, *Nanotoxicology* **2014**, 8, 295-304.

[55] K. Fent, C. J. Weisbroda, A. Wirth-Heller, U. Pieles, *Aquat. Toxicol.* **2010**, *100*, 218-228.

[56] T. C. K. Heiden, E. Dengler, W. J. Kao, W. Heideman, R. E. Peterson, *Toxicol. Appl. Pharm.* **2007**, *225*, 70-79.

[57] A. H. Cory, T. C. Owen, J. A. Barltrop, J. G. Cory, *Cancer Commun.* **1991,** *3*, 207-212.

Table of Contents